Am J Physiol Cell Physiol 287: C673–C681, 2004.
First published May 5, 2004; 10.1152/ajpcell.00044.2004.

Fiber type and temperature dependence of inorganic phosphate: implications for fatigue

E. P. Debold, H. Dave, and R. H. Fitts

Department of Biological Sciences, Marquette University, Milwaukee Wisconsin 53201

Submitted 23 January 2004; accepted in final form 22 April 2004

Debold, E. P., H. Dave, and R. H. Fitts. Fiber type and temperature dependence of inorganic phosphate: implications for fatigue. *Am J Physiol Cell Physiol* 287: C673–C681, 2004. First published May 5, 2004; 10.1152/ajpcell.00044.2004.—Elevated levels of P_i are thought to cause a substantial proportion of the loss in muscular force and power output during fatigue from intense contractile activity. However, support for this hypothesis is based, in part, on data from skinned single fibers obtained at low temperatures (≤15°C). The effect of high (30 mM) P_i concentration on the contractile function of chemically skinned single fibers was examined at both low (15°C) and high (30°C) temperatures using fibers isolated from rat soleus (type I fibers) and gastrocnemius (type II fibers) muscles. Elevating P_i from 0 to 30 mM at saturating free Ca^{2+} levels depressed maximum isometric force (P_o) by 54% at 15°C and by 19% at 30°C ($P < 0.05$; significant interaction) in type I fibers. Similarly, the P_o of type II fibers was significantly more sensitive to high levels of P_i at the lower (50% decrease) vs. higher temperature (5% decrease). The maximal shortening velocity of both type I and type II fibers was not significantly affected by elevated P_i at either temperature. However, peak fiber power was depressed by 49% at 15°C but by only 16% at 30°C in type I fibers. Similarly, in type II fibers, peak power was depressed by 40 and 18% at 15 and 30°C, respectively. These data suggest that near physiological temperatures and at saturating levels of intracellular Ca^{2+}, elevated levels of P_i contribute less to fatigue than might be inferred from data obtained at lower temperatures.

skinned single fiber; force; power

REPEATED HIGH-FREQUENCY STIMULATION of muscle results in a rapid decline in muscular force and power, with the degree of change dependent on the duration and intensity of activity as well as on the fiber type composition of the muscle (2, 17). The decline in force has been demonstrated to strongly correlate with an increase in muscle P_i concentration (7, 44, 50). Although the strength of the correlation varies (1), in the later stages of fatigue, when maximal isometric force is depressed by >70%, the intracellular P_i concentration can exceed 30 mM compared with the 1–5 mM level in resting fibers (44). These observations suggest that P_i may play a causative role in fatigue.

Skinned single muscle fiber studies provide convincing evidence that elevations in P_i depress maximum isometric force (P_o) in a concentration-dependent manner (9–11, 18, 28, 30–32, 38). Notably, Potma et al. (38) observed a 55% decline in P_o after increasing P_i from 0 to 30 mM at 15°C in chemically skinned rabbit soleus fibers. Even larger P_i-induced reductions in P_o were observed in psoas myofibrils (43) and in single fibers when the initial P_i concentration was reduced to ~5 μm with the use of a P_i mopping enzyme system (36). High levels of P_i are thought to reduce force by reversing the P_i release/force-generating step by mass action (22). Taken together with in vivo NMR data (7, 50), the single-fiber experiments provide compelling evidence that elevated P_i participates in the loss of muscular force during fatigue. However, the single-fiber results were obtained at temperatures far below mammalian physiological values (10–15°C), making it difficult to apply the findings directly to in vivo muscle fatigue.

It is now well established that muscle contractile properties are temperature sensitive, with P_o, V_{max}, and peak power increasing significantly as temperature is increased (39–41). Furthermore, Zhao and Kawai (52) and Wang and Kawai (45) suggested that the rate constants of the cross-bridge cycle may be differentially temperature sensitive. In particular, the forward rate constant of force generation is increased by temperature by a greater amount than the backward rate constant. In contrast, elevated P_i is thought to reduce force by increasing the backward rate constant (22). If the temperature effect is greater than the effect of fatiguing levels of P_i, the depressive effects of P_i may be reduced at physiological temperatures. Skinned single fibers deteriorate rapidly when exposed to physiological temperatures; thus reliable data have traditionally been difficult to obtain at higher temperatures.

Dantzig et al. (13) provided the first evidence that the P_i effect is temperature dependent. They observed a reduced effect at 20 vs. 10°C in skinned rabbit psoas fibers; however, the highest temperature used was still well below mammalian physiological temperatures. More recently, techniques have been developed to examine the effects of elevated P_i at near physiological temperatures in chemically skinned fibers (12, 33, 37, 42, 45, 52). Most notably, Coupland et al. (12) observed that rabbit psoas fibers were less sensitive to elevated P_i at temperatures near mammalian physiological values (32.5°C). Increasing P_i by 25 mM reduced P_o by 50% at 10°C but by only 16% at 30°C, suggesting that the effects of P_i on P_o are minimized near physiological temperatures. However, these studies focused solely on P_o, while the effects on the force-velocity relationship and power were not examined. Because movement is dependent on power, the effect of P_i on this parameter is potentially the most relevant measure for understanding fatigue (2, 17).

Skeletal muscles are heterogeneous, composed of slow type I and fast type II fibers, and it is well documented that the latter fatigue more rapidly. Therefore, to understand the role of P_i in muscular fatigue, its effects must be quantified in both fiber types. However, publications to date have focused on fibers from either predominantly fast or slow muscle, with few studies incorporating both fiber types. Investigators who have examined the effects of P_i on P_o in fibers from slow and fast muscle have observed conflicting results, with elevated P_i having no fiber type dependence (38, 47) or preferentially affecting fast (30, 43) or slow fiber types (18).

Address for reprint requests and other correspondence: E. P. Debold, Dept. of Molecular Physiology and Biophysics, Univ. of Vermont, 149 Beaumont Ave., Rm. 112, Burlington, VT 05401 (E-mail: ndebold@physiology.med.uvm.edu).

The costs of publication of this article were defrayed in part by the payment of page charges. The article must therefore be hereby marked "*advertisement*" in accordance with 18 U.S.C. Section 1734 solely to indicate this fact.

While single fibers in these investigations were isolated from muscles that contained a high percentage of one fiber type, only one study characterized the myosin heavy chain (MHC) with the use of gel electrophoresis (47); thus the results could be contaminated by fibers expressing the minority MHC profile. In addition, these studies were performed at well below physiological temperatures. The purpose of the present study was to determine the effects of elevated P_i level on contractile function in both slow type I and fast type II fibers at near physiological temperatures. By determining the effect of high P_i on peak power, these experiments provide more conclusive evidence regarding the role of P_i in fatigue during intense contractile activity. The results demonstrate that P_o was reduced by a significantly greater amount at 15°C than at 30°C in both type I and type II fibers. Although maximum shortening velocity, V_{max} [as determined from the Hill plot of the force-velocity data (23)], was not significantly affected by elevated P_i at either temperature, peak fiber power was reduced twice as much at 15°C as at 30°C. Nonetheless, the P_i-induced decline in peak power was significant in slow and fast fibers at both temperatures. Preliminary results from these data were previously published in abstract form (14).

METHODS

Solutions. The composition of relaxing (pCa 9.0) and activating (pCa 4.5) solutions were derived with an iterative computer program (15) by using the stability constants contained within the program (16) and adjusting for temperature, pH, and ionic strength. All solutions contained (in mM) 20 imidazole, 7.0 ethylene glycol-bis(β-aminoethyl ether)-*N*,*N*,*N*′,*N*′-tetraacetic acid (EGTA), 4 MgATP, and 14.5 creatine phosphate. Calcium was added as $CaCl_2$, and ATP was added as a disodium salt. P_i was added as K_2HPO_4 to yield a total concentration of either 5 or 30 mM, and the amount of anion was adjusted to maintain ionic strength. Although no P_i was added to the 0 mM condition, it is thought that the actual concentration was between 0.5 and 0.7 mM in the fibers of slow and fast muscle, respectively (34), owing to contamination from the hydrolysis and regeneration of ATP in addition to impurities in the added creatine phosphate. Mg^{2+} was added in the form of $MgCl_2$ with a specified free concentration of 1 mM. Each solution had an ionic strength of 180 mM, which was controlled by varying the amount of KCl added, and was raised to pH 7.0 with KOH. The skinning solution was composed of 50% relaxing solution and 50% glycerol (vol/vol). In addition, before each fiber was tested, it was submerged into a Brij 58 solution (50 mg/10 ml of relaxing solution polyoxyethylene 20 cetyl ether; Sigma) for 30 s to disrupt any remaining intact membranes after exposure to the skinning solution.

Single-fiber preparation. Male Sprague-Dawley rats (Sasco, Madison, WI) were anesthetized with pentobarbital sodium (50 mg/kg body wt ip), after which the soleus and the gastrocnemius were removed and placed in a 4°C relaxing solution. The rats were subsequently killed with a pneumothorax while still heavily anesthetized. The protocol for animal care and disposal was approved by the university's Institutional Animal Care and Use Committee and followed the guidelines of the National Institutes of Health.

Each muscle was dissected into small bundles (~1 mm in width) and tied to glass capillary tubes. For the gastrocnemius, bundles were prepared from the superficial region of the medial head (a visually white region containing a high percentage of fast type IIb and IIx fibers and denoted white gastrocnemius) and the deep region of the lateral head (a visually red region containing a high percentage of fast type IIa fibers and denoted red gastrocnemius). Bundles were stored in skinning solution at 4°C for the first 24 h, after which the solution was replaced by fresh skinning solution and the bundles were stored at −20°C until used but not longer than 4 wk.

On the day of experiment, fiber bundles were removed from the skinning solution and placed in a 4°C relaxing solution. A single-fiber segment was isolated from a bundle and then transferred to an ~500-μl glass-bottomed chamber in a milled stainless steel plate. This plate was modified to incorporate a chamber that was cooled to 15°C by Peltier cells at one end and a second chamber at the opposite end, which was heated with an electrically powered heat-controlling unit to 30°C. The chambers were separated by a 3-cm plastic insulator to maintain the temperature differential. The stainless steel plate was supported by leaf springs, allowing the plate to be manually depressed. Once depressed, with the fiber briefly suspended in air, the plate could be shifted horizontally to move the second chamber underneath the exposed fiber. Once in position, the plate was allowed to rise, bringing the fiber into the solution bath of the second chamber.

The ends of each fiber were secured between a force transducer (Cambridge model 400A; Cambridge Technology, Watertown, MA) and a servomotor (Cambridge model 300B) as previously described (48).

The stainless steel plate was secured to the stage of an inverted microscope, allowing the fiber to be viewed at ×800. Sarcomere length was adjusted to 2.5 μm using a calibrated eyepiece micrometer. Fiber length was determined by measuring the distance between the points of attachment. Fiber diameter was measured by taking a Polaroid photograph while the fiber was briefly suspended in air. The width of the fiber was measured at three points along the length of the fiber segment, and the average value was used to calculate the diameter, assuming the fiber is circular (29).

Experimental design. The contractile properties measured in slow type I and fast type II fibers included P_o, V_{max}, and force-velocity and force-power relationships at 15 and 30°C. In the initial set of experiments with slow type I fibers, the fiber was exposed to 0 and 30 mM P_i using a repeated-measures design such that each fiber tested was subjected to both temperatures at both P_i concentrations. The order of conditions was balanced across P_i concentrations such that an equal number of fibers was initially exposed to 30 and 0 mM P_i. This method was used to control for potential order effects caused by exposure to 30 mM P_i. However, the fiber was always exposed to the 15°C condition first because of the tendency for the higher temperature to damage the fiber. Type II fibers were more unstable near physiological temperatures; thus a strict repeated-measures design could not be used. A mixed design was used for type II fibers in which one group of fibers was subjected to low and high P_i at 15°C, while a separate set of fibers was exposed to low and high P_i at 30°C.

Because it has been suggested that the resting P_i in type I fibers is closer to 6 mM (27), an additional set of experiments was performed during which type I fibers were exposed to 5 and 30 mM added P_i. The second set of experiments was also performed with a repeated-measures design. The order of exposure to low (5 mM) and elevated (30 mM) P_i levels was balanced such that the first fiber was initially exposed to 5 mM P_i concentration and the second fiber was first exposed to 30 mM P_i. This design was used to control for any possible order effect that the elevated P_i might have had on the contractile properties.

For data collection at 15°C, the fibers were maintained in a 15°C relaxing solution between contractions. During data collection at the higher temperature (30°C), the fibers were maintained in a 15°C relaxing solution between brief (2–5 s) contractions in a high-temperature activating solution (Fig. 1). The diffusion coefficient for P_i has been reported to be 2.1×10^{-6} cm^2/s (33); therefore, 2–5 s should have provided adequate time for diffusion of P_i into the depths of a 70- to 90-μm fiber. Maintaining the fibers in a cold relaxing solution between contractions allowed for reliable data to be obtained at the elevated temperatures. Other investigators (33, 37) have suggested that fibers perform best when they are initially activated at cold temperatures before being moved into the higher-temperature activating solution. However, in our work, this method did not affect the stability of either slow or fast fibers and thus was not used.

Once the fiber was mounted and set to optimal length, P_o was taken as the peak level of force achieved while the fiber was submerged in

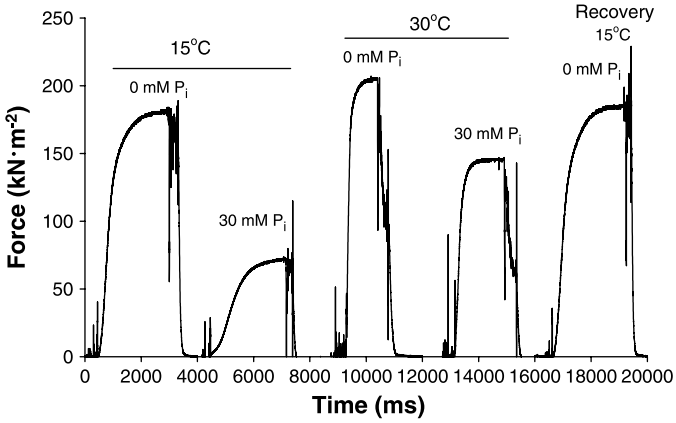

Fig. 1. Representative maximum isometric force data from a soleus type I muscle fiber. The fiber was sequentially activated by exposure to 4 different high Ca^{2+} (pCa 4.5) solutions: 15°C and 0 mM P_i, 15°C and 30 mM P_i, 30°C and 0 mM P_i, and 30°C and 30 mM P_i. P_o was determined as the peak force attained during the steady-state plateau in force in each condition. Between each activation, the fiber was placed in a 15°C relaxing solution (pCa 9.0) during which the force returned to baseline, which caused the movement artifact observed at the beginning and end of each force trace. A final force record was obtained at 15°C and 0 mM P_i (recovery) to demonstrate that the fiber was not damaged by contracting at 30°C (recovery trace).

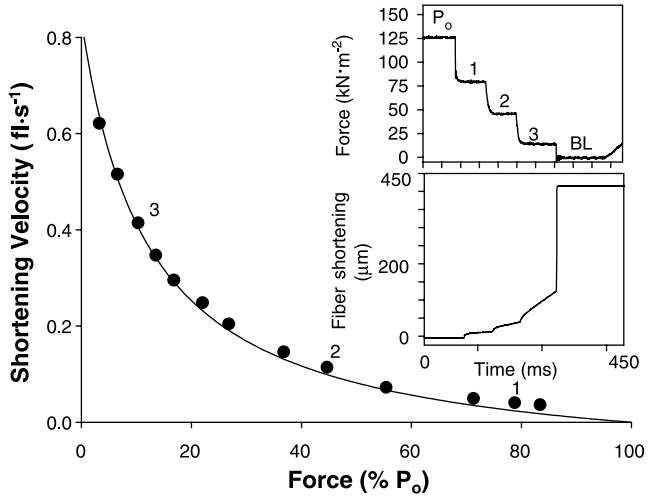

Fig. 2. Force-velocity relationship, showing fiber velocity plotted as a function of the percentage of maximum isometric force (%P_o). *Insets* depict sample traces of force (*top*) and shortening (*bottom*) during a maximal contraction in which the fiber was switched from P_o to 3 isotonic loads. The fiber shortened at velocities necessary to maintain fiber force at 3 predetermined levels. Finally, the fiber was rapidly slacked to 400 μm, and force dropped to the baseline (BL). During the second half of each load clamp, both force and velocity were measured from the force and position traces, respectively. The force and velocity values from the *insets* are labeled *1*, *2*, and *3* in the main graph. Five contractions, each including 3 load-clamped values, were performed, and the values were plotted and fit with the Hill equation (23) using an iterative nonlinear curve-fitting procedure (Marquardt-Levenberg algorithm). These data represent values obtained at 15°C and without added P_i. Shortening velocity is in units of fiber length per second, and force is represented as %P_o. Total fiber shortening ranged from 15 to 18% of initial length.

activating solution, as depicted in Fig. 1. Fibers were excluded from the analysis if the maximal isometric force dropped below 90% of the initial P_o at each condition. V_{max} was determined for each fiber by activating it in pCa 4.5. After attainment of steady force (~2–5 s), fibers were subjected to a series of isotonic loads, and the data were fit with the Hill equation,

$$(P + a)(V + b) = (P_o + a)b$$

where P is isometric force, V is velocity, a is a constant with units of force, and b is a constant with units of velocity (23). For individual fibers, shortening velocity (slope of the best-fit line of the position trace) and relative force were determined during the last half of each isotonic load step (Fig. 2). These data were fit to the Hill equation with the use of an iterative nonlinear curve-fitting procedure (Marquardt-Levenberg algorithm) as previously described (49). Peak fiber power was calculated with the fitted parameters of the force-velocity curve and P_o (49). Composite force-velocity and force-power curves were constructed by summating velocities or power values from 0 to 100% of P_o in increments of 1%.

Fiber type classification. The MHC composition of the fibers was determined by SDS gel electrophoresis. After the contractile measurements, each fiber was solubilized in 10 μl of 1% SDS sample buffer and stored at −80°C. To establish the MHC profile, the fibers were run on 5% polyacrylamide gels (wt/vol) and silver stained as described previously (20). This procedure enabled type I fibers to be distinguished reliably from type II fibers by visual assessment. Although there are three different isoforms of MHC type II expressed in rat fibers, the molecular weights of the type IIx and IIb isoforms are very similar and not reliably distinguished with gel electrophoresis. Thus all type II fibers were considered as a single group. On the basis of visual inspection of the gel, fibers were classified as having MHC type I or type II.

Statistical analysis. A repeated-measures ANOVA model was used to determine whether a significant interaction existed between the main effects of temperature and P_i concentration for all contractile properties measured in type I fibers. For type II fibers, a mixed design was used, with one between factor (temperature) and one within factor (P_i concentration). The significance level for all analyses was set at $P < 0.05$. In addition, a mixed design (two within factors and one between factor) was used to compare the differences among the different fiber types. A Tukey's honestly significant difference post hoc test was used to locate any specific differences not immediately apparent from the ANOVA model. All analyses were performed using Statistica for Windows, release 5.1 (Statsoft, Tulsa, OK).

RESULTS

Figure 1 depicts representative force traces from a type I fiber sequentially exposed to 0 and 30 mM P_i at both temperatures. Increasing the temperature caused P_o to increase, while elevating the P_i concentration from 0 to 30 mM depressed force at both temperatures. The final force record in Fig. 1 demonstrates that the fiber was undamaged by the maximal contraction at the high temperature, evidenced by the ability of the fiber to produce force equal to that observed in the initial control condition (15°C and 0 mM P_i).

Table 1. *Effects of P_i and temperature on maximal isometric force*

		Force, kN/m²					
		15°C			30°C		
MHC Type	*n*	0 mM P_i	30 mM P_i	%Δ	0 mM P_i	30 mM P_i	%Δ
II	14, 23	125±15	63±9*	↓50	174±23†	165±21‡	↓5
I	18	135±26	62±17*	↓54	178±41†	144±31*‡	↓19

Values are means ± SD; *n* refers to sample size. Differences were considered significant at $P < 0.05$. The two values for *n* for type II fibers represent separate groups of fibers for 15 and 30°C, respectively. Force values are expressed relative to cross-sectional area, and type refers to the isoform of myosin heavy chain (MHC) content of the fibers. %Δ indicates the relative difference in force between 0 and 30 mM added P_i. *Significant main effect for [P_i]. †Significant temperature main effect. ‡Significant temperature by [P_i] interaction.

Table 2. *Effect of condition order on maximum isometric force*

Initial [P_i], mM	*n*	P_o, kN/m^2 15°C, 0 mM P_i	15°C, 30 mM P_i	30°C, 0 mM P_i	30°C, 30 mM P_i
0	9	122±38	60±17	167±55	133±22
30	9	122±21	50±20	162±42	133±23

Values are means ± SD. Maximum isometric force (P_o) is depicted for each condition as a function of the initial [P_i] to which the fiber was exposed for type I fibers. The initial condition to which the fiber was first exposed is depicted in the first column. ANOVA model did not reveal any significant differences between the starting conditions.

Table 1 summarizes the effects of increasing P_i from 0 to 30 mM at 15 and 30°C on P_o across both fiber types. P_o expressed relative to the cross-sectional area of the fiber was not significantly different between the two fiber types at either the low or the high temperature. P_o was significantly increased at the higher temperature, with Q_{10} values of 1.2 and 1.3 for type I and type II fibers, respectively. At the lower temperature, P_o was significantly reduced by the addition of 30 mM P_i in both fiber types, but at the higher temperature, P_o was significantly reduced only in type I fibers. Because of the differing experimental designs used for the two fiber types, a strict statistical comparison of the effects of P_i on P_o across fiber types was not performed. In addition, because of different ATPase activities, the level of contamination is inherently larger for fast type II fibers (13). However, examination of the means reveals that at the lower temperature, both fiber types appeared to be equally sensitive to P_i, but at the higher temperature, type I fibers were almost four times more sensitive than type II fibers to P_i. Regardless of fiber type, the magnitude of the P_i-induced reduction in P_o demonstrated temperature dependence, with the reductions always being significantly greater at the lower vs. the higher temperature.

Because the same slow type I fiber was exposed to both 0 and 30 mM P_i in the repeated-measures design, it was possible that one condition might affect the subsequent condition, particularly when the 0 mM P_i condition followed the 30 mM P_i condition. The balanced repeated-measures design controlled for any potential order effects. However, the existence of an order effect can still be determined by comparing the P_o values in fibers initially exposed to 0 mM P_i with those initially exposed to 30 mM P_i. The analysis revealed that the effects of P_i were independent of the initial P_i concentration (Table 2), indicating the lack of an effect on the previous condition.

The mean effects of P_i on force-velocity parameters are summarized in Tables 3 and 4 for type I and type II fibers, respectively. Figure 3 shows representative force-velocity curves for a single slow type I fiber exposed to all four conditions, with raw force and position traces displayed in Fig. 3, *insets*. The mean force-velocity relationship is shown in Fig. 4. Increasing the temperature in control conditions increased V_{max} 5.6- and 2.3-fold in slow and fast fibers, respectively, while the increase in P_i did not significantly affect this parameter. At the higher temperature, the force-velocity relationship was shifted to the right and exhibited less curvature, as evidenced by the higher a/P_o value (Tables 3 and 4). Thus, not only were P_o and V_{max} increased at 30°C, but the amount of force produced at any given velocity was also higher at the higher temperature. The 30 mM P_i caused a leftward shift in the force-velocity relationship such that at any given velocity, less force was produced by the fiber (Fig. 4). This shift was more pronounced at the lower than at the higher temperature in both fiber types, and it was not evident when force was expressed relative to $\%P_o$ in each condition (Fig. 4, *insets*). The latter indicates that the shift in the force-velocity relationship was solely due to the reduction in P_o. The effect of P_i on the curvature of the force-velocity relationship was temperature dependent. In both fiber types, 30 mM P_i had little effect at 15°C but significantly decreased the a/P_o value at 30°C (Tables 3 and 4). The effects of P_i on peak fiber power were temperature dependent. At 15°C, 30 mM P_i reduced peak type I fiber power by 49%, while at 30°C the reduction was only 26% ($P < 0.05$; a significant interaction). A similar temperature dependence was observed for the fast type II fibers, in which high P_i reduced peak power by 40 and 18% at 15 and 30°C, respectively. Composite force-power curves generated from the mean data are shown in Fig. 5, *A* and *B*. Elevating the temperature from 15 to 30°C without added P_i caused peak fiber power to increase roughly 20- and 7-fold for slow and fast fibers, respectively. In addition, increasing the temperature (i.e., without added P_i) caused peak power to occur at a significantly greater shortening velocity and force level in both types I and II fibers (Tables 3 and 4). This is visually apparent in the main graphs in Fig. 4 (velocity) and Fig. 5 (peak power). Elevated P_i significantly reduced peak power in both fiber types at both temperatures; however, the depressive effect was significantly greater at the lower temperature in both fiber types (Tables 3 and 4 and Fig. 5).

For slow fibers, a final set of experiments was conducted to compare the effects of increasing the P_i from 5 mM, a typical resting value for slow fibers, to 30 mM. These data were qualitatively similar to the findings derived from comparing the effects of raising the P_i level from 0 to 30 mM. Elevating the P_i from 5 to 30 mM caused a 25% reduction in P_o at 15°C but only a 14% reduction at 30°C. As expected, V_{max} was not

Table 3. *Summary of effects of P_i and temperature of contractile parameters of type I fibers*

[P_i], mM	Temp, °C	V_{max}, fl/s	a/P_o	Power, kN·m^{-2}·fl·s^{-1}	V_{opt}, fl/s	P_{opt}, kN/m^2
0	15	0.92±0.43	0.08±0.03	4.7±1.6	0.19±0.01	27.0±1.0
30	15	0.75±0.31	0.12±0.10	2.4±0.9*	0.17±0.01	14.4±0.8*
0	30	5.20±0.52†	0.44±0.15†	106.3±24.0†	1.82±0.04†	62.7±1.3†
30	30	5.26±0.95†	0.31±0.17*†‡	78.7±26.2*†‡	1.70±0.06†	47.2±1.8*†

Values are means ± SD. Mean force-velocity parameters for type I fibers were measured at 15 and 30°C and with 0 and 30 mM P_i. *Significantly different from 0 mM P_i. †Significant main effect for temperature under the corresponding P_i (0 or 30 mM P_i). ‡Significant temperature-P_i interaction. V_{max} was obtained by fitting the force-velocity data to the Hill force-velocity equation (see Fig. 2). V_{opt} indicates the shortening velocity at which peak power occurred. P_{opt} indicates the force at which peak power occurred.

Table 4. *Summary of effects of P_i and temperature of contractile parameters of type II fibers*

[P_i], mM	Sample *n*	Temperature, °C	V_{max}, fl/s^{-1}	a/P_o	Power, kN·m^{-2}·fl·s^{-1}	V_{opt}, fl/s^{-1}	P_{opt}, kN/m^2
0	12	15	2.64±1.02	0.14±0.06	20.2±5.6	0.65±0.22	31.1±3.5
30		15	2.93±0.77	0.15±0.08	12.2±5.8*	0.76±0.24	18.1±7.9*
0	14	30	6.13±0.79†	0.45±0.13†	136.3±30.0†	2.20±0.45†	64.6±7.1†
30		30	7.02±1.71†	0.28±0.13*†‡	112.3±31.6*†‡	2.18±0.37	53.9±11.0*†

Values are means ± SD. Mean force-velocity parameters for type II fibers were measured at 15 and 30°C and with 0 and 30 mM P_i. *Significantly different from 0 mM P_i. †Significant main effect for temperature at corresponding P_i (0 or 30 mM P_i). ‡Significant temperature-P_i interaction. V_{max} was obtained by fitting the force-velocity data to the Hill force-velocity equation (see Fig. 2). V_{opt} indicates the shortening velocity at which peak power occurred. P_{opt} indicates the force at which peak power occurred.

affected at either temperature by the 25 mM increase in P_i. However, peak power was reduced by a significantly greater amount at 15 vs. 30°C. The relative reductions in peak power caused by increasing P_i from 0 to 30 and from 5 to 30 mM at both temperatures are summarized in Table 5. At 15°C, the reductions in peak power were larger when P_i was increased from 0 to 30 mM than when it was increased from 5 to 30 mM, while no difference in the %depression was observed at 30°C (Table 5).

DISCUSSION

Our results indicate that *1*) high P_i significantly reduced types I and II fiber P_o and peak power at low temperatures and all but type II fiber P_o at high temperatures, and *2*) the reduction in these variables was significantly less at 30°C than it was at 15°C. Thus, at saturating levels of intracellular Ca^{2+}, increased muscle P_i during in vivo exercise would depress force and power less than previously expected on the basis of force measurements at 15°C.

The magnitude of the P_i-induced reduction in P_o observed at 15°C in the present study agrees with those previously observed in rat fibers under similar conditions in fast (12, 38) and slow muscle fibers (38). Furthermore, the temperature-dependent P_i effect is consistent with the data of Dantzig et al. (13) and Coupland et al. (12), who observed a decreased effect of high P_i on peak force as temperature increased from 10 to 20°C and from 2.5 to 32.5°C, respectively. The present findings extend these observations by including the characterization of

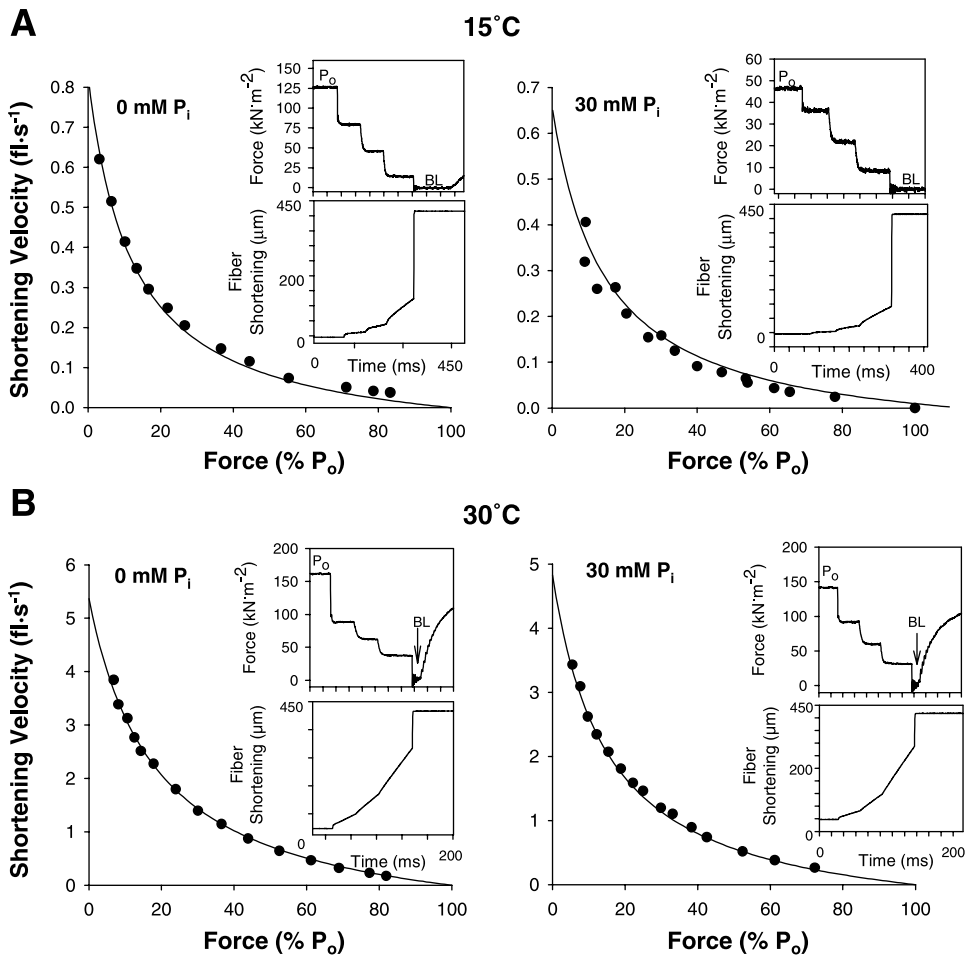

Fig. 3. Representative force-velocity curves and raw force and displacement (shortening) records from a soleus type I fiber under all 4 experimental conditions. Force-velocity relationships were derived by exposing a single type I fiber to each of the 4 different activating solutions (pCa 4.5) using the methods described in Fig. 2. *Top insets* depict representative force, *bottom insets* depict position traces, and main graphs depict the fitted force-velocity curve for 0 and 30 mM P_i at 15°C (*A*) and 30°C (*B*). P_o indicates maximal isometric force obtained before the first of 3 isotonic loads. BL indicates baseline force level, which occurred after the final isotonic load. Note the different time scales used in the *insets* for data obtained at 15 vs. 30°C.

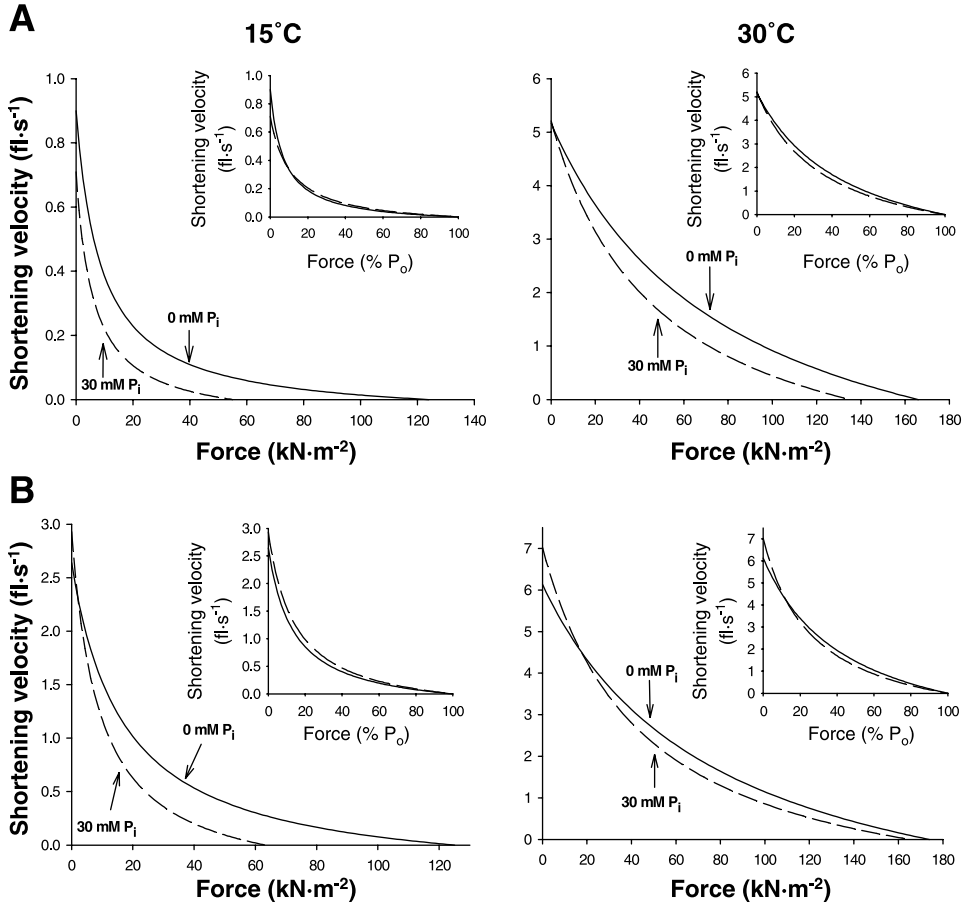

Fig. 4. Composite force-velocity curves at 15 and 30°C for soleus type I muscle fibers (*A*) and gastrocnemius type II muscle fibers (*B*). Shortening velocity is plotted as a function of force in kilonewtons per square meter (main graphs) and as a function of $\%P_o$ (*insets*). The solid lines represent 0 mM P_i, while the dashed lines represent data obtained with 30 mM P_i added. Graphs at *left* are from data obtained at 15°C, while the graphs at *right* are derived from data obtained at 30°C. The curves were constructed by calculating velocity values at each force level from 0 to 100% of mean P_o in 1% increments. The individual points were removed, leaving the line connected through the center of each point.

P_i effects on the force-velocity and force-power relationships for both type I and type II fibers. Our results are inconsistent with those of Tesi et al. (43), who observed the effects of P_i to be temperature independent in both fast and slow myofibrils. However, these authors used much lower temperatures to compare the effects of P_i, 5 vs. 15°C in rabbit fast (psoas) and 15 and 20°C in slow (soleus) myofibrils. This finding suggests that the temperature dependence of P_i on force may occur only below and above some critical temperature, as was suggested for maximal shortening velocity (37).

Muscle contraction against a load produces movement through the generation of power, as evidenced during exercise modalities such as running and bicycling. Therefore, the most important measure for determining muscular performance is peak power. Often, investigators reporting studies involving single fibers have drawn conclusions about performance on the basis of an ion's effects on maximal isometric or unloaded contractions (10, 31). P_o and V_{max} represent two extremes on the continuum of the force-velocity relationship, and peak power typically occurs between 20 and 40% of P_o; thus it is imperative to examine the complete force-velocity relationship to best understand the causes of fatigue.

Because high P_i is thought to be an important contributor to fatigue during intense exercise, the observed temperature dependence of P_i on contractile function has important implications (17). The present findings demonstrate that at saturating Ca^{2+} levels (pCa 4.5), the role of P_i in reducing muscular force and power output is less at temperatures approaching physiological values. Indeed, in type I fibers, the P_i-induced depression in P_o was two to three times greater than, and the reduction in peak power was almost twice as great as, at the lower temperature compared with the higher temperature. In type II fibers, the temperature effect was even greater, with the effects of P_i on P_o being 10 times greater at 15 vs. 30°C.

The temperature-dependent effect of P_i observed in the present study is qualitatively similar to that observed by Pate et al. (33) for H^+ (pH). They demonstrated a >50% reduction in the effect of lowering pH from 7.0 to 6.2 in skinned fibers at 30 vs. 10°C. This is not surprising, because elevations in H^+ and P_i are both thought to reduce force by affecting the force-generating step of the cross-bridge cycle (26), thus suggesting that temperature dependence is mediated by a similar mechanism (see below). If increases in H^+ and P_i were found to act independently to reduce force, these ions would account for only one-half to one-fourth of the reduction that might be predicted from studies at lower temperatures. Furthermore, extrapolating the effects to 38°C, a typical human in vivo limb muscle temperature during exercise (25), one could predict that elevated levels of P_i and H^+ would exert even smaller changes.

The a/P_o ratio increased with temperature in both fast and slow fibers. This suggests that at physiological temperatures, muscle fibers produce more force at a given velocity. The reduced curvature of the force-velocity relationship (higher a/P_o ratio) at physiological temperature also contributed to increased peak power (39).

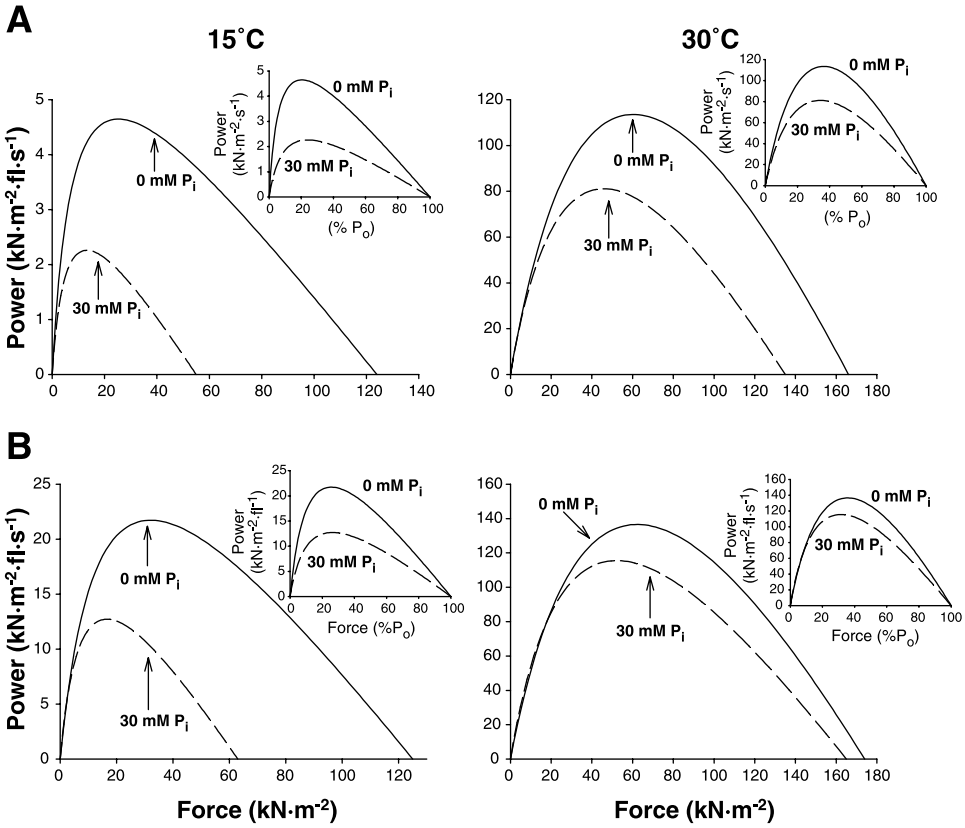

Fig. 5. Composite force-power curves at 15 and 30°C for soleus type I muscle fibers (*A*) and gastrocnemius type II muscle fibers (*B*). Power is plotted as a function of force in kilonewtons per square meter (main graphs) and as a function of $\%P_o$ (*insets*). The solid lines represent 0 mM P_i, and the dashed lines represent 30 mM P_i. Graphs at *left* are from data obtained at 15°C, while the graphs at *right* are derived from data obtained at 30°C. The curves were constructed by calculating power values at each force level from 0 to 100% of the mean P_o in 1% increments. The individual points were removed, leaving the line connected through the center of each point.

In the present study, we observed that at higher velocities (the initial ascending side of the force-power curve), P_i had no effect on power in either fiber type and was evident at 15 or 30°C (Fig. 5). Because P_i had no effect on V_{max}, it is not surprising that the high-velocity, low-force contractions were unaltered. In terms of fatigue, this observation implies that low-force, high-velocity contractions would be unaffected by elevated levels of P_i. It should be noted that in both slow and fast fibers, peak power was significantly reduced by P_i at the higher temperatures, indicating that elevated levels of P_i do play a significant role in the depression of muscular function during intense physical activity. However, the magnitude of the reduction in P_o and peak power at 30°C was far smaller than the declines observed in vivo after intense contractile activity (7, 50). These findings imply that other factors implicated in the fatigue process have greater responsibility for the decline in muscular performance.

The present data appear contradictory to previous findings in in vivo muscle that demonstrated strong relationships between the buildup of P_i and fatigue during intense contractile activity (7, 50). However, there are several changes in addition to the increase in P_i that could potentially explain the dramatic loss of muscular performance resulting from high-intensity contractile activity. A decrease in intracellular pH has been the best-studied ionic change correlated with the onset of fatigue. Recent evidence suggests only a small role for elevated protons in fatigue (33); however, combined elevations in P_i and H^+ have not been examined at near physiological temperatures. It is possible, therefore, that elevated levels of these ions act synergistically to depress muscle function during fatigue.

Another observation that has received considerable attention is the reduction in sarcoplasmic reticulum (SR) Ca^{2+} release and the amplitude of the Ca^{2+} transient in the later stages of fatigue (46). The reduced amplitude of the Ca^{2+} transient appears to result in part from an increase in SR P_i, which precipitates with SR Ca^{2+}, thereby reducing the amount of free Ca^{2+} available for release into the myoplasm (3, 18). Elevated levels of P_i have also been shown to decrease the Ca^{2+} sensitivity of rabbit psoas fibers at lower temperatures (28). Thus, when intracellular [Ca^{2+}] declines, muscular force may be further reduced by the decreased Ca^{2+} sensitivity caused by elevated P_i. However, the effects of increased P_i on Ca^{2+} sensitivity have not been determined for any fiber type at physiological temperatures. Therefore, to fully determine the role of P_i during each stage of fatigue, it is necessary to examine the effects of elevated P_i on the force-pCa relationship at near physiological temperatures.

At 30°C, type II fiber P_o and the force-power relationship were less sensitive to P_i than those of the slow type I fibers. Previous work examining the effects of elevated P_i concentra-

Table 5. *Comparison of effects of increasing P_i from either 0 or 5 to 30 mM on peak power in soleus type I fibers*

Increase in [P_i], mM	Temperature, °C	Decrease in Peak Fiber Power, %
0 vs. 30	15	48
5 vs. 30	15	35
0 vs. 30	30	25*
5 vs. 30	30	26*

Comparison of the mean %decrease in peak type I fiber power after increasing P_i from either 0 or 5 mM to 30 mM at both 15 and 30°C. *Decrease in peak fiber power at 30°C is significantly less than decrease at 15°C.

tion on different fiber types has yielded contradictory results. Our results regarding the effects on P_o at 15°C agree with those of Potma et al. (38), who found no difference in the P_i sensitivity of force in rat fibers from fast and slow muscle at the same temperature. However, the present findings (at 15°C) disagree with those in two previous studies in which fibers from fast muscle were observed to be less sensitive than fibers from slow muscle (4, 18, 45). Similarly, Godt and Nosek (21) observed that cardiac muscle fibers (which possess the same β-MHC isoform as slow skeletal muscle fibers) had greater sensitivity to P_i than the predominately fast fibers of rabbit psoas muscle. Millar and Homsher (30), in contrast, observed that rabbit psoas fibers had greater P_i sensitivity than soleus fibers at P_i concentrations >10 mM. Although the reason for these contradictory findings is not readily apparent, several factors in these studies varied and may account for the discrepancies. One possibility is that the previous studies failed to classify the isoforms of MHC present. Thus it is possible that the responses observed by previous authors contained both type I and type II fibers. In addition, the findings are also complicated by the fact that each study used different experimental temperatures, and the present results indicate that the effects of elevated P_i on a particular fiber type depend on the temperature. Our results show type II fibers to be less sensitive to P_i at high temperatures but not at low temperatures. This may be related to kinetic differences between the fiber types. Wang and Kawai (45), using sinusoidal analysis, observed that the Q_{10} for several rate constants of the cross-bridge cycle were dependent on the fiber type studied.

The mechanism of the temperature-dependent effect of P_i on P_o, present in both fiber types, is not clear; however, it may be due to the differential temperature sensitivity of the steps in the cross-bridge cycle (13, 45, 52). It is generally thought that elevated P_i reduces P_o by decreasing the proportion of cross bridges in the force-producing states (22, 35, 36). On the basis of sinusoidal analysis in fibers from both fast (52) and slow (45) muscle, it was suggested that the forward rate constant of the force-generating step is more temperature sensitive than the reverse rate constant. Ranatunga (42) observed a similar phenomenon in using a laser temperature jump technique while examining the effects of P_i on rate constants of force redevelopment. Therefore, at a higher compared with a lower temperature, the cross bridge spends a relatively greater proportion of the cycle strongly bound to actin, an effect attributed in part to the regulatory proteins (19). This hypothesis predicts an increase in P_o as temperature is elevated, as several authors have observed (33, 41, 52). Applying this hypothesis to the present data suggests that the effects of temperature on the forward rate constant of force generation outpaced the effects of added P_i on the reverse rate constant. In other words, the increase in temperature had a stronger impact than the elevation in P_i on the equilibrium constant of the force-generating step. This hypothesis may also explain the temperature dependence of pH on P_o in skinned fibers because elevated levels of protons are also thought to affect the force-generating step of the cross-bridge cycle (26). This model, however, assumes that increasing the P_i depresses force by decreasing the fraction of strongly bound cross bridges. Alternatively, experiments in which a spin label is used on the mobile region of the light chain domain of myosin have suggested that added P_i does not affect the distribution of strongly bound cross bridges (5), implying that the force exerted by a cross bridge is lowered at high P_i. In addition, it is possible that elevated fiber force with increasing temperature is in part due to an increase in the force per cross bridge. Xu et al. (51) observed temperature to increase the helical order of the myosin head and hypothesized that this would reduce the internal drag, producing a faster filament sliding velocity. While the increased filament order might contribute to the temperature effect on fiber velocity and thus peak power, whether it exerts any effect on force is not known. It is not clear from the present data which model is correct, and the possibility exists that both might play a role. However, the theory that temperature and P_i have competing effects on the rate constants of the force-generating step is the simplest interpretation, because it does not require an altered force per cross bridge. This theory could also explain the observation that elevating temperature increased the a/P_o ratio. An increased forward rate constant of the force-generating step would allow for a higher percentage of attached cross bridges at any given shortening velocity.

Our finding that fast fibers were more fragile than slow fibers is consistent with other published data, and the effect has been observed at both low (8) and high (45) temperatures. Although the reason for this difference remains unexplained, it was recently suggested that differing amounts of intermediate filaments among fast and slow muscle may explain the fiber type dependence of structural integrity (8). These filaments are thought to be important in maintaining the three-dimensional structure of the sarcomere while the fiber is contracting (6). Similarly, the differences in stability may be explained by the increased amount of α-actinin present in the Z-band structure of slow type I fibers (24).

In summary, elevating P_i has a significantly greater effect on single-fiber P_o and power at 15 vs. 30°C. Thus it appears that the role of an increase in P_i in muscular fatigue at saturating levels of Ca^{2+} is smaller than previously hypothesized. To better understand the cause of muscle fatigue, future work should assess the combined effects of increased P_i and H^+ and reduced intracellular free Ca^{2+} on peak force and power.

ACKNOWLEDGMENTS

We thank Janell Romatowski for help in performing the MHC isoform analyses, and, posthumously, Nick Schook for work in designing and machining the temperature jump used in these experiments. We also thank Stephanie Jones for helping to prepare the manuscript.

Present address of E. P. Debold: Dept. of Molecular Physiology and Biophysics, University of Vermont, Burlington, VT 05401.

GRANTS

This work was supported in part by National Aeronautics and Space Administration Grant NAG 9-1156 (to R. H. Fitts).

REFERENCES

1. **Adams GR, Fisher MJ, and Meyer RA.** Hypercapnic acidosis and increased $H_2PO_4^-$ concentration do not decrease force in cat skeletal muscle. *Am J Physiol Cell Physiol* 260: C805–C812, 1991.
2. **Allen DG, Lannergren J, and Westerblad H.** Muscle cell function during prolonged activity: cellular mechanisms of fatigue. *Exp Physiol* 80: 497–527, 1995.
3. **Allen DG and Westerblad H.** Role of phosphate and calcium stores in muscle fatigue. *J Physiol* 536: 657–665, 2001.
4. **Altringham JD and Johnston IA.** Effects of phosphate on the contractile properties of fast and slow muscle fibers from an Antarctic fish. *J Physiol* 368: 491–500, 1985.

5. **Baker JE, LaConte LEW, Brust-Mascher I, and Thomas DD.** Mechanochemical coupling in spin-labeled, active, isometric muscle. *Biophys J* 77: 2657–2664, 1999.
6. **Boriek AM, Capetanaki Y, Hwang W, Officer T, Badshah M, Rodarte J, and Tidball JG.** Desmin integrates the three-dimensional mechanical properties of muscles. *Am J Physiol Cell Physiol* 280: C46–C52, 2001.
7. **Cady EB, Jones DA, and Moll A.** Changes in force and intracellular metabolites during fatigue of human skeletal muscle. *J Physiol* 418: 327–337, 1989.
8. **Campbell KS and Moss RL.** History-dependent mechanical properties of permeabilized rat soleus muscle fibers. *Biophys J* 82: 929–943, 2002.
9. **Chase PB and Kushmerick MJ.** Effects of pH on contraction of rabbit fast and slow skeletal muscle fibers. *Biophys J* 53: 935–946, 1988.
10. **Cooke R, Franks K, Luciani G, and Pate E.** The inhibition of rabbit skeletal muscle contraction by hydrogen ions and phosphate. *J Physiol* 395: 77–97, 1988.
11. **Cooke R and Pate E.** The effects of ADP and phosphate on the contraction of muscle fibers. *Biophys J* 48: 789–798, 1985.
12. **Coupland ME, Puchert E, and Ranatunga KW.** Temperature dependence of active tension in mammalian (rabbit psoas) muscle fibres: effect of inorganic phosphate. *J Physiol* 536: 879–891, 2001.
13. **Dantzig JA, Goldman YE., Millar NC, Lacktis J, and Homsher E.** Reversal of the cross-bridge force-generating transition by photogeneration of phosphate in rabbit psoas muscle fibers. *J Physiol* 451: 247–278, 1992.
14. **Debold EP and Fitts RH.** The effects of temperature and P_i on single muscle fiber contractile properties (Abstract). *Biophys J* 78: 119A, 2000.
15. **Fabiato A.** Computer programs for calculating total from specified free or free from specified total ionic concentrations in aqueous solutions containing multiple metals and ligands. *Methods Enzymol* 157: 378–417, 1988.
16. **Fabiato A and Fabiato F.** Calculator programs for computing the composition of the solutions containing multiple metals and ligands used for experiments in skinned muscle cells. *J Physiol (Paris)* 75: 463–505, 1979.
17. **Fitts RH.** Cellular mechanisms of muscle fatigue. *Physiol Rev* 74: 49–94, 1994.
18. **Fryer MW, Owen VJ, Lamb GD, and Stephenson DG.** Effects of creatine phosphate and P_i on Ca^{2+} movements and tension development in rat skinned skeletal muscle fibers. *J Physiol* 482: 123–140, 1995.
19. **Fujita H and Kawai M.** Temperature effect on isometric tension is mediated by regulatory proteins tropomyosin and troponin in bovine myocardium. *J Physiol* 539: 267–276, 2002.
20. **Giulian GG, Moss RL, and Greaser M.** Improved methodology for analysis and quantitation of proteins on one dimensional silver-stained slab gels. *Anal Biochem* 129: 277–287, 1983.
21. **Godt RE and Nosek TM.** Changes of intercellular milieu with fatigue or hypoxia depress contraction of skinned rabbit skeletal and cardiac muscle. *J Physiol* 413: 155–180, 1989.
22. **Hibberd MG, Dantzig JA, Trentham DR, Goldman YE.** Phosphate release and force generation in skeletal muscle fibers. *Science* 228: 1317–1319, 1985.
23. **Hill AV.** The heat of shortening and the dynamic constants of muscle. *Proc R Soc B* 126: 136–195, 1938.
24. **Jones DA and Round JM.** *Skeletal Muscle in Health and Disease: A Textbook of Muscle Physiology*. New York: Manchester University Press, 1990, p. 60–61.
25. **Kenny GP, Reardon FD, Zaleski W, Reardon ML, Haman F, and Ducharme MB.** Muscle temperature transients before, during, and after exercise measured using an intramuscular multisensor probe. *J Appl Physiol* 94: 2350–2357, 2003.
26. **Kentish JC.** Combined inhibitory actions of acidosis and phosphate on maximum force production in rat skinned cardiac muscle. *Pflügers Arch* 419: 310–318, 1991.
27. **Kushmerick MJ, Moerland TS, and Wiesman RW.** Mammalian skeletal muscle fibers distinguished by contents of phosphocreatine, ATP, and P_i. *Proc Natl Acad Sci USA* 89: 7521–7525, 1992.
28. **Martyn DA and Gordon AM.** Force and stiffness in glycerinated rabbit psoas fibers: effects of calcium and elevated phosphate. *J Gen Physiol* 99: 795–816, 1992.
29. **Metzger JM and Moss RL.** Shortening velocity in skinned single muscle fibers. Influence of filament lattice spacing. *Biophys J* 52: 127–131, 1987.
30. **Millar NC and Homsher E.** Kinetics of force generation and phosphate release in skinned rabbit soleus fibers. *Am J Physiol Cell Physiol* 262: C1239–C1245, 1992.
31. **Nosek TM, Fender KY, and Godt RE.** It is diprotonated inorganic phosphate that depresses force in skinned skeletal muscle fibers. *Science* 236: 191–193, 1987.
32. **Nosek TM, Leal-Cardoso JH, McLaughlin M, and Godt RE.** Inhibitory influence of phosphate and arsenate on contraction of skinned skeletal and cardiac muscle. *Am J Physiol Cell Physiol* 259: C933–C939, 1990.
33. **Pate E, Bhimani M, Franks-Skiba K, and Cooke R.** Reduced effect of pH on skinned rabbit psoas muscle mechanics at high temperatures: implications for fatigue. *J Physiol* 486: 689–694, 1995.
34. **Pate E and Cooke R.** Addition of phosphate to active muscle fibers probes actomyosin states within the powerstroke. *Pflügers Arch* 414: 73–81, 1989.
35. **Pate E and Cooke R.** A model of crossbridge action: the effects of ATP, ADP and P_i. *J Muscle Res Cell Motil* 10: 181–196, 1989.
36. **Pate E, Franks-Skiba K, and Cooke R.** Depletion of phosphate in active muscle fibers probes actomyosin states within the powerstroke. *Biophys J* 74: 369–380, 1998.
37. **Pate E, Wilson GJ, Bhimani M, and Cooke R.** Temperature dependence of the inhibitory effects of orthovanadate on shortening velocity in fast skeletal muscle. *Biophys J* 66: 1554–1562, 1994.
38. **Potma EJ, van Graas IA, and Stienen GJ.** Influence of inorganic phosphate and pH on ATP utilization in fast and slow skeletal muscle fibers. *Biophys J* 69: 580–2589. 1995.
39. **Ranatunga KW.** The force-velocity relation of rat fast- and slow-twitch muscles examined at different temperatures. *J Physiol* 351: 517–529, 1984.
40. **Ranatunga KW.** Endothermic force generation in fast and slow mammalian (rabbit) muscle fibers. *Biophys J* 71: 1905–1913, 1996.
41. **Ranatunga KW.** Temperature dependence of mechanical power output in mammalian (rat) skeletal muscle. *Exp Physiol* 83: 371–376, 1998.
42. **Ranatunga KW.** Effects of inorganic phosphate on endothermic force generation in muscle. *Proc R Soc Lond B Biol Sci* 266: 1381–1385, 1999.
43. **Tesi C, Colomo F, Piroddi N, and Poggesi C.** Characterization of the cross-bridge force-generating step using inorganic phosphate and BDM in myofibrils from rabbit skeletal muscles. *J Physiol* 541: 187–199, 2002.
44. **Thompson LV, Balog EM, Riley DA, and Fitts RH.** Muscle fatigue in frog semitendinosus: alterations in contractile function. *Am J Physiol Cell Physiol* 262: C1500–C1506, 1992.
45. **Wang G and Kawai M.** Effect of temperature on the elementary steps of the cross-bridge cycle in rabbit soleus slow-twitch muscle fibers. *J Physiol* 531: 219–234, 2001.
46. **Westerblad H, Lee JA, Lannergren J, and Allen DG.** Cellular mechanisms of fatigue in skeletal muscle. *Am J Physiol Cell Physiol* 261: C195–C209, 1991.
47. **Widrick JJ.** Effect of inorganic phosphate on the unloaded shortening velocity of slow and fast mammalian fibers. *Am J Physiol Cell Physiol* 282: C647–C653, 2002.
48. **Widrick JJ, Knuth ST, Norenberg KM, Romatowski JG, Bain JLW, Riley DA, Karhanek K, Trappe SW, Trappe TA, Costill DL, and Fitts RH.** Effect of a 17 day spaceflight on contractile properties of human soleus fibers. *J Physiol* 516: 915–930, 1999.
49. **Widrick JJ, Trappe SW, Costill DL, and Fitts RH.** Force-velocity and force-power properties of single muscle fibers from elite master runners and sedentary men. *Am J Physiol Cell Physiol* 271: C676–C683, 1996.
50. **Wilson JR, McCully KK, Mancini DM, Boden B, and Chance B.** Relationship of muscular fatigue to pH and diprotonated P_i in humans: a ^{31}P-NMR study. *J Appl Physiol* 64: 2333–2339, 1988.
51. **Xu S, Offer G, Gu J, White HD, and Wu LC.** Temperature and ligand dependence of conformation and helical order in myosin filaments. *Biochemistry* 42: 390–401, 2003.
52. **Zhao Y and Kawai M.** Kinetic and thermodynamic studies of the cross-bridge cycle in rabbit psoas muscle fibers. *Biophys J* 67: 1655–1668, 1994.